NANO LETTERS

2008
Vol. 8, No. 2
661−667

Chemically Induced Permanent Magnetism in Au, Ag, and Cu Nanoparticles: Localization of the Magnetism by Element Selective Techniques

José S. Garitaonandia,*,† Maite Insausti,† Eider Goikolea,† Motohiro Suzuki,‡ John D. Cashion,§ Naomi Kawamura,‡ Hitoshi Ohsawa,‡ Izaskun Gil de Muro,† Kiyonori Suzuki,|| Fernando Plazaola,† and Teofilo Rojo†

Zientzia eta Teknologia Fakultatea. Euskal Herriko Unibertsitatea, 644pk. 48820 Bilbao, Spain, Japan Synchrotron Radiation Research Institute (JASRI/Spring-8) 1-1-1 Kouto, Mikazuki, Sayou 679-5198, Japan, School of Physics, Building 27, Monash University, Victoria 3800, Australia, and Department of Materials Engineering, Building 19, Monash University, Victoria 3800, Australia

Received November 30, 2007; Revised Manuscript Received January 8, 2008

ABSTRACT

We report a direct observation of the intrinsic magnetization behavior of Au in thiol-capped gold nanoparticles with permanent magnetism at room temperature. Two element specific techniques have been used for this purpose: X-ray magnetic circular dichroism on the L edges of the Au and ^{197}Au Mössbauer spectroscopy. Besides, we show that silver and copper nanoparticles synthesized by the same chemical procedure also present room-temperature permanent magnetism. The observed permanent magnetism at room temperature in Ag and Cu dodecanethiol-capped nanoparticles proves that the physical mechanisms associated to this magnetization process can be extended to more elements, opening the way to new and still not-discovered applications and to new possibilities to research basic questions of magnetism.

The ultimate aim of the current nanotechnology is the development and design of materials and systems at the nanometric scale with controlled properties suitable to a concrete application. The success of this task requires the development of mechanical−physical and chemical procedures to get systems with great stability and homogeneity and with desired shapes and compositions. Presently, modern lithography equipments allow the manipulation and the creation of structures even at atomic level.[1] In the same way, by means of the new methods of chemical syntheses, other important advances have been achieved in this field as, for example, the stabilization of regular structures formed by nanoparticles of different magnetic behaviors of even less than 2 nm[2].

Apart from the logical technological limits, there is another handicap that must be faced: the innate limits imposed by the physics and chemistry of the nanomaterials. As the size of the material decreases, properties presented in bulk materials cloud due to the increasing importance of the relative dispersion of the sizes or, even, disappear as a consequence of the incompatibility of the size with the property as, for instance, the ferromagnetism in magnetic metallic nanoparticles.

In a nanometric scale, two important factors regulate the properties of a material: (a) the size effect, due to the increasing confinement of the electrons as the size of a particle decreases down to values comparable to the wavelength of an electron at the Fermi level, and (b) the surface effect, as a consequence of the relative increase of the surface atoms with different chemical and structural topology.

These two effects have a great influence in the total energy of the system and condition its final structure and shape. Because most of the atoms of the nanomaterial are located at the surface, the surface atoms play a crucial role in the energy minimization and, consequently, in the stabilization

* Corresponding author. E-mail: garita@we.lc.ehu.es.
† Euskal Herriko Unibertsitatea.
‡ Japan Synchrotron Radiation Research Institute (JASRI/Spring-8).
§ School of Physics, Monash University.
|| Department of Materials Engineering, Monash University.

10.1021/nl073129g CCC: $40.75
Published on Web 01/24/2008

of the system.[3,4] The minimization of the energy includes changes in the charge distributions that can differ from the surface to the bulk due to the quantum confinement of the electrons.[5,6]

A way to obtain metallic nanoparticles (NP) is the capping of the NPs by means of functional groups such as amines,[7] phosphine,[8] alcohols,[9] thiols,[10] or even certain acids[11] that interact with the surface atoms preventing the particle growth.[10] This method allows the stabilization of nanoparticles of less than 2 nm presenting other additional advantages, such as size control and a narrow size distribution, which has greatly popularized its use as a way to obtain monodispersed nanosized nuclei of different elements, compositions, and capping for different technological applications and studies.

Special interest has been aroused by the influence of the capping on the properties of the NPs. It has been observed that properties such as optical response,[12] magnetism,[13,14] or reactivity[15] can differ significantly from their bare or bulk counterparts with these changes being modulated by the chemical affinity of the capping group to the surface atoms of the metallic NP.

For example, certain metals, amine, or alcohol groups interact weakly with the atoms at the surface and preserve the electronic properties, including the surface ones, of a bare NP. On the other extreme, thiols interact strongly with atoms at the surface and induce significant charge redistribution and the consequent change in the physical properties.[5,16]

Thiol-capped Au NPs represent a good example of this effect. In these nanoparticles, 5d electrons of the Au atoms can be involved in the electron redistribution as a consequence of the size effect, causing a hybridation with the 6s electron and locating them close to the Fermi energy level. The strong affinity between the Au surface atoms and the S atoms of the thiols induces a strong charge transfer from the Au surface atoms to the S atoms where the participation of 5d electrons can be also implied. As a direct consequence, unoccupied densities of d states located at the Au surface atoms are generated, making these atoms susceptible to becoming magnetic.[5,6]

This fact has been corroborated by some experiments that verify the step from diamagnetism to a magnetic state for the Au NPs. However, surprisingly, a great variety of effects going from giant paramagnetism,[17] superparamagnetism,[18] and even permanent magnetism[19,20] have been reported from thiol-capped Au NPs synthesized by similar chemical routes and apparently with similar structures, sizes, or compositions.

Aside from the fact that it is a gold NP that has become magnetic, the nature of the permanent magnetism is amazing in two different ways. On one hand, the macroscopic magnetic signal hardly varies with the temperature over a wide range up to room temperature. On the other hand, permanent magnetism is present for sizes that in any other system would be superparamagnetic. The microscopic confirmation of this fact would mean an invaluable step for the physics of the magnetism. It would involve the possible existence of magnetism over superparamagnetic limits of the bare metallic NPs, opening the way to new and still not-discovered applications and to new possibilities to research basic questions of magnetism.

Two main questions are hidden behind these results: is the origin of the magnetism really located on the Au atoms? And if it is so, are there more elements susceptible to induce magnetism on them?

We have tackled these two questions in an independent way. First, we have synthesized dodecanothiol-capped NPs of three different elements: Au, Ag, and Cu. For that, we have followed the well-known Brust method taking special care of the initial parameters of the synthesis to intensify the effect of the dodecanothiol on the surface of the particles.[10,21] Second, we centered our efforts in the microscopic magnetic characterization of the Au NPs.

TEM micrographs and particle size distribution histograms for the dodecanothiol-capped Au, Ag, and Cu nanoparticles have been performed (Figure 1). In the three samples, face-centered cubic (fcc) crystal structure was identified with higher lattice parameters than those presented in their corresponding bulk samples.[21] The size distribution histograms disclose similar main particle sizes ($\sim$2 nm) and narrow size distributions ($\sim$0.2 nm) for the three characterized Au, Ag, and Cu NPs. More detailed figures can be consulted in Table 1.

Macroscopic magnetization measurements have been performed at 5 and 300 K by a SQUID magnetometer (Quantum Design) (Figure 2). Several facts must be underlined from this figure: (a) the clear saturation of the magnetic signals of the three samples even at 300 K (except for the Cu at 5 K as will be later discussed), (b) the preservation of the magnetic signal from 5 to 300 K (only a decrease of $\sim$10% is observed), (c) the similarity between the magnetic behaviors of the Au and Ag NPs and among the coercive fields of the three samples ($\sim$190 Oe at 5 K and $\sim$80 Oe at 300 K), and (d) the outstanding value of the saturation magnetization up to 5 emu/gr for the Ag and Au NPs and up to two magnitude orders higher than other previously published values for similar NPs.[11,18−20,22]

After the macroscopic magnetization measurements, the samples were checked for magnetic impurities by inductively coupled plasma mass spectroscopy (ICP−MS). Fe traces ($\leq$1 ppm) were found in all the samples. This amount, nevertheless, certainly cannot justify the magnetization observed macroscopically and even can affect in such a way the magnetic properties of the Au. Besides, it has been probed that the presence of Fe in the Au NPs weakens the magnetism of the NPs by delocating the charge from the surface of the NPs.[23] The grade of location or itinerancy of the surface charge in NPs has been usually weighed up by the intensity of the band on the ultraviolet−visible part of the spectrum associated to the so-called surface plasmon resonance.[24] In the case of the Au, Ag, and Cu NPs studied in this paper, this band was completely absent confirming the localization of the charge at the surface of the NPs.[21]

A complete microscopic magnetic characterization has been performed on the Au NPs. Several reasons drove us to select the NPs of this element. On one hand, previously published papers related to the Au NPs afford us valuable

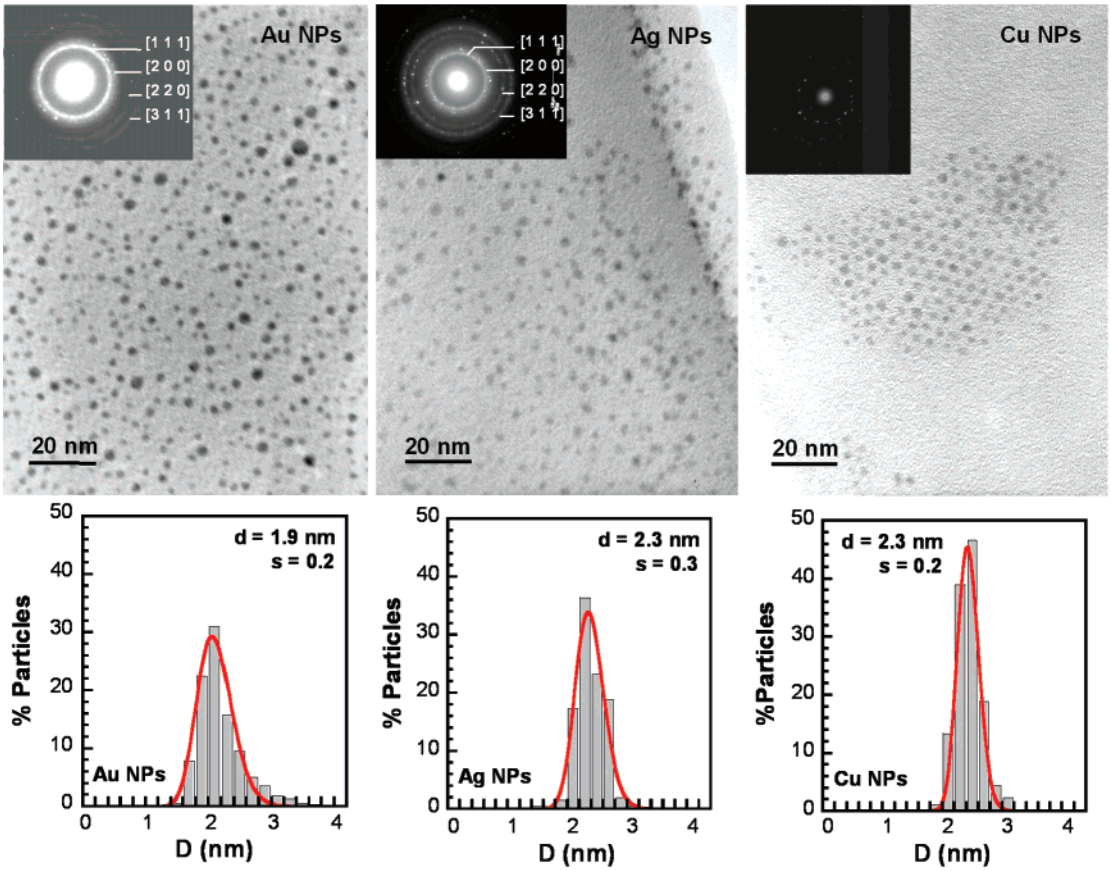

Figure 1. Transmission electron micrographs of Au, Ag, and Cu nanoparticles capped by dodecanothiol (above) and their corresponding size distributions histograms (below). The solid line represents the fitting curve assuming a log-normal function. The calculated mean particle diameter (d) and the standard deviation (σ) are shown in the histograms.

Table 1. Summary of the Structural and Magnetic Characteristics of the Au, Ag, and Cu Dodecanothiol-Capped NPs Studied in This Paper

	mean size (nm)[a]	weight of the organic component[b]	number of shells[c]	magnetization (emu/g metal)[d]	Mr/Ms (at RT)[e]	magnetization (μB/magnetic atom)[f]	ratio surface metal/S[g]
Au NP	1.9 ± 0.2	15%	3	6.0	0.077	0.33	1:0.27
Ag NP	2.3 ± 0.3	22%	4	7.4	0.072	0.27	1:0.30
Cu NP	2.3 ± 0.2	30%	4	2.8	0.056	0.06	1:0.37

[a] Mean sizes and deviations as calculated from the fitting of the distribution histograms presented in Figure 1. [b] Relative weight of dodecanothiol determined from thermogravimetry and ICP analysis. [c] Number of fcc-structured shells for the different NPs estimated from the mean sizes and lattice parameters. [d] Magnetization values calculated from the magnetization curves at 5 K. [e] Remanence to saturation magnetization ratio obtained from curves at 5 K. [f] Magnetic moments of the surface magnetic atoms estimated from magnetization results and the relative quantity of surface atoms in the NPs. [g] Relative quantity of surface metal atoms to S atoms as estimated from thermogravimetry and ICP analysis.

data that could be compared and discussed with those obtained from our measurements. In addition, Au NPs allow us to use element selective techniques such as X-ray magnetic circular dichroism (XMCD) and ^{197}Au Mössbauer spectroscopy, which is not available for the Ag and Cu elements. The combined use of these two techniques provides different and complementary microstructural magnetic information on a particular element.

It has been observed that the X-ray absorption structure (XAS) of the Au atoms of the thiol-capped Au NPs present an intensity increase of the resonance at the threshold (whiteline) associated with a $2p_{3/2}$ to $5d_{5/2,\ 3/2}$ dipole transition with respect to the bare Au metal that probes the existence of unoccupied d states in the Au atoms at the Fermi level.[5,6] The XMCD technique allows us to monitor the magnetic behavior of these transitions and to obtain element specific magnetization (ESM) measurements evaluating the difference between the absorptions of the sample to the right and left circularly polarized X-ray under a magnetic field.

Figure 3 shows the XAS and XMCD spectra of the Au nanoparticles at the L_3 edge ($2p_{3/2} \rightarrow 5d_{5/2}\ 6s_{1/2}$ allowed dipolar transition) and L_2 edge ($2p_{1/2} \rightarrow 5d_{3/2}\ 6s_{1/2}$) where the 5d electrons come into play. The spectra were obtained at room temperature and in applied magnetic field of 10 T. Two different XMCD signals with an order of magnitude of 10^{-5} of the XAS step height are clearly observed at both L_3 and L_2 edges. One of these signals is centered at ~11.928 keV (L_3) and at ~13.748 keV (L_2), and its sign changes when the magnetic field is reversed, which verifies the magnetic origin of this contribution.

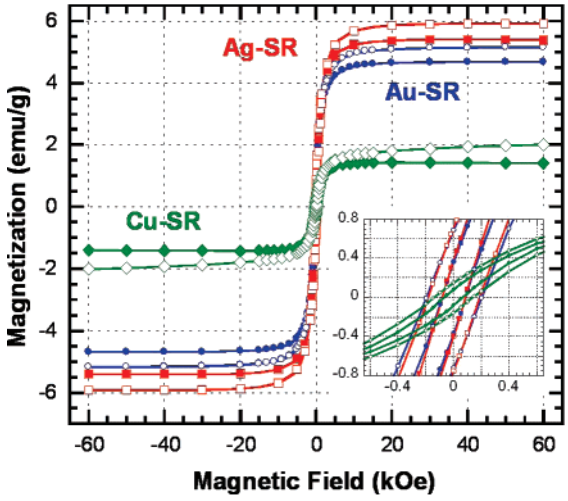

Figure 2. Magnetization curves of the Au, Ag, and Cu dodecanothiol-capped NPs. Open symbols represent measurements obtained at 5 K and filled symbols measurements obtained at 300 K. The similar coercive fields at 300 and 5 K and for the Au, Ag, and Cu NPs can be noticed in the inset.

Associated with this last contribution, an ESM measurement was obtained at room temperature by considering the XMCD signal as proportional to the magnetization and gathering the amplitude of the signal at the L_3 edge as a function of the external magnetic field (Figure 4). The ESM shows a clear hysteretic behavior with the applied magnetic field, a distinguishable coercivity (see inset in Figure 4), and a tendency to saturation above 5 kOe, similar to those observed in the macroscopic magnetization measurements (Figure 2).

Mössbauer spectroscopy is an element selective technique based on γ-energy recoilless nuclear resonance, property only observed in nuclei of isotopes of certain elements. This technique is characterized by its high sensitivity to local physical and chemical changes, suitable for microstructural and magnetic characterization of samples and alloys.

Figure 5 shows the ^{197}Au Mössbauer spectrum of the dodecanothiol-capped Au NPs. Two different contributions can be observed. The main one is a single line centered at −0.26 mm/s (all isomer shifts are quoted with respect to Au metal) and a width of 2.0 mm/s, only slightly larger than the 1.9 mm/s of the Au calibration foil. This contribution is from the fcc Au core of the NPs and it is clearly nonmagnetic. The isomer shift (IS) is within the range of values found for the core of Au_{55} molecular clusters.[25] The negative IS is caused by the decrease of the average electron density at the nuclei of these Au nuclei as a consequence of lattice expansion.[26]

The second one is a split component centered on positive values and stems from the surface Au atoms. As it is known, the loss of symmetry with respect to the inner atoms and the existence of chemical bonds of different nature can cause high electric field gradients and changes in the electron densities in the nuclei of the surface atoms.[26−28] This fact is clearly reflected in the quadrupolar splitting (QS) and IS values of the spectral components of these atoms. Studies reported in the literature on the relation of the capping with the QS and IS values of the surface Au atoms of different NPs reveal that these atoms change the valence state to Au(I).[29] No fitting of the split component of the spectrum shown in Figure 5 achieves values for IS and QS that could directly relate the surface Au atoms to either Au(I) valence state nor any valence state of the Au found in the literature.[30] So, taking into account the XMCD and ESM results, we have considered this component as an unresolved magnetic splitting, smaller than the quadrupole splitting and oriented at a powder-averaged, random angle to the electric field gradient. It has been theoretically calculated and probed experimentally that magnetically split ^{197}Au Mössbauer spectra show eight different transitions with well-determined relative intensities.[31] These intensities were fixed during the fitting procedure. Under the last considerations, an IS of 3.55 mm/s, a QS value of −4.3 mm/s, a hyperfine field of 9.0 T, and a width of 2.0 mm/s were obtained. Although magnetic hyperfine fields have been observed previously in ferromagnetic gold alloys, the fields in those cases have been due to conduction electron polarization transferred from an alloyed, magnetic, 3d element. This is the first time that a hyperfine field has been observed due to a magnetic moment resident on the gold atom.

The relative intensity of the magnetic subspectrum was 40%, much less than the 63% of the atoms on the surface in a particle formed by three fcc structured shells of Au atoms as expected from the size of here studied Au NPs. However, the spectral area must be corrected for the difference in the bonding strength of core and surface atoms, which changes the recoilless fraction of the gamma ray absorption. Using the values obtained by Smit el al.[32] for the surface and core atoms in a two atom radius Au_{55} molecule produced an expected, weighted subspectrum value of 53%. This an important point because, although the agreement is not perfect, the difference of the magnetic subspectrum from anything seen previously in the literature[26,29] and its combination with the XMCD and ESM results unquestionably locates the magnetism of these NPs on the surface Au atoms.

After determining the location of the magnetic atoms in the NPs, the logical next step is to calculate their magnetic moments. The relative weight of the organic (dodecanothiol) component in the NPs was calculated by ICP−MS and thermogravimetry. The thermogravimetry technique provided us an independent physical way to estimate the relative weight of the organic component. Moreover, it allows observing the stability of the NPs with regard to the temperature, too. The degradation and the subsequent volatilization of the organic capping were detected at ∼500 K. The relative decrease of the measured weights were consistent with those calculated from ICP−MS results and lay from 15% for Au NPs up to 30% for Cu ones as it can seen in Table 1. Taking into account the particle sizes obtained from TEM images, it can be considered that the Au NPs are formed by three fcc shells and the Ag and Cu ones by four shells, which raises the relative quantity of surface atoms in the NPs up to 63 and 52%, respectively. These data in conjunction with the saturation magnetization values obtained from the M(H) curves at 5 K lead to values

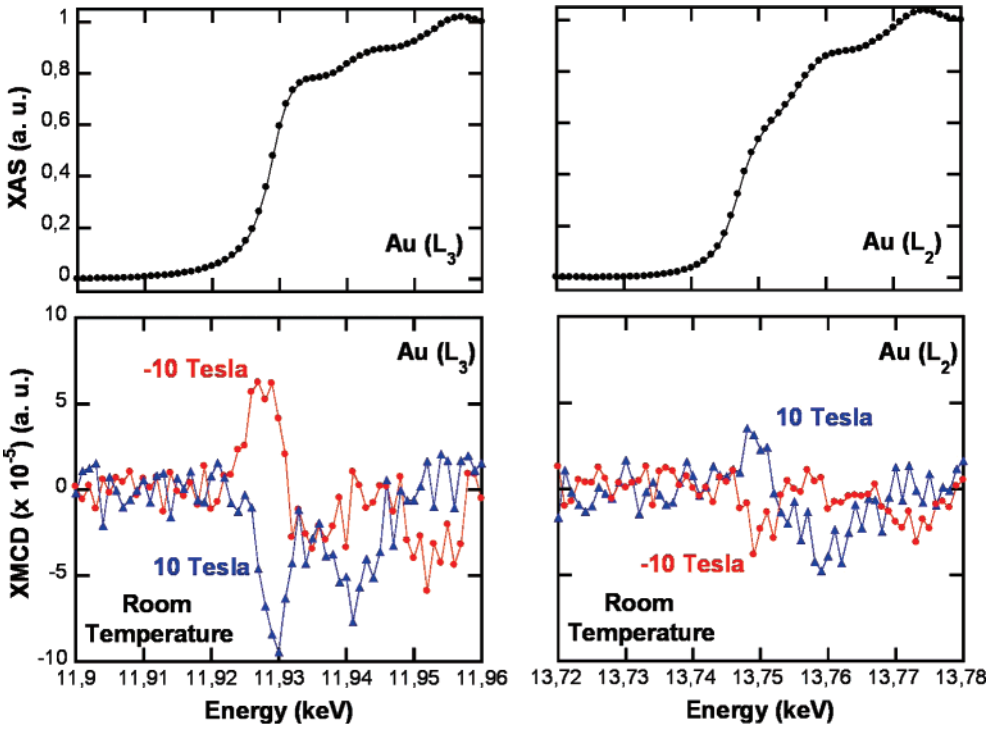

Figure 3. XMCD and XAS spectra obtained at the Au L_3 and L_2 edge with applied magnetic field of 10 T. XMCD spectra have been normalized taking into account a branching ratio of 2:1 in the dipole transition for L_3 and L_2 edges.

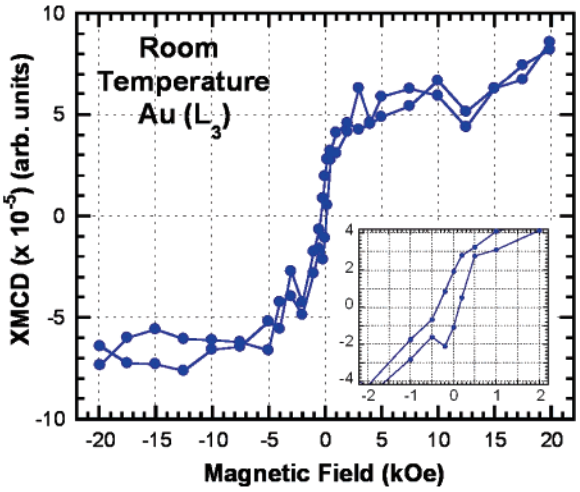

Figure 4. ESM of dodecanothiol-capped Au NPs obtained from the amplitude of the XMCD spectra at the Au L_3 edge as a function of the applied magnetic field. The coercivity of the ESM is clearly observed in the inset.

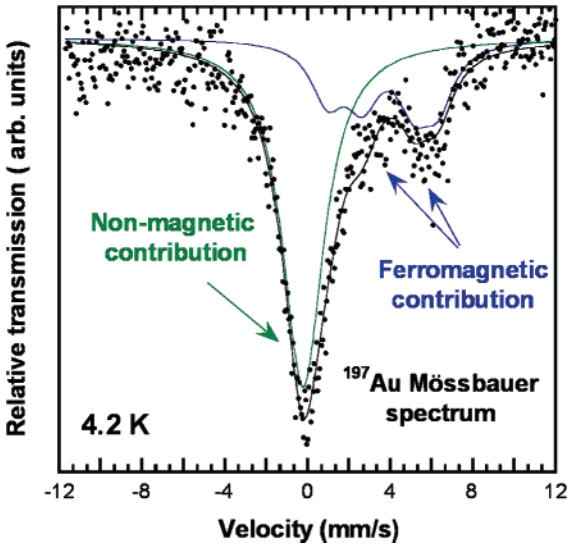

Figure 5. ^{197}Au Mössbauer spectrum of dodecanothiol-capped Au NPs at 4.2 K. The spectrum has been fitted by a nonmagnetic singlet contribution corresponding to the inner Au atoms with a fcc structure and a ferromagnetic one from the surface Au atoms.

of magnetic moments of ~0.3 μ_B for the surface atoms in the Au and Ag NPs and ~0.06 μ_B in the Cu ones. The notable difference between the magnetic moments calculated for the Au and Ag magnetic atoms and for the Cu magnetic ones is due to the presence of diamagnetic Cu_2O and antiferromagnetic CuO in the Cu NPs as it can be perceived in the hysteresis curve of these NPs obtained at 5 K (see Figure 2). We could not avoid the oxidation of part of the Cu in any of our trials. However, it has been observed that CuO nanoparticles present Neel temperatures of ~40 K[33], and therefore the saturated magnetic signal observed in the hysteresis loops at room temperature would be due exclusively to the dodecanothiol-capped Cu NPs.

The persistence of an almost invariable magnetism even at temperatures above 300 K in these NPs is a clear indication of the high local anisotropy associated with the magnetism of the dodecanothiol-capped Au, Ag, and Cu atoms. A simple calculation of the anisotropy constants corresponding to 2 nm size NPs with blocking temperatures above 300 K shows values up to 10^9 J/m^3 or 0.4 eV per atom.[34] This huge anisotropy can be compared with that observed on the surface layers of thin films of thiol-capped Au.[17] As in the Au, Ag, and Cu thiol-capped NPs, the lack of symmetry on the surface of the film and the charge transfer from surface metal

atoms to S atoms define a covalent and strong located directional bond. This feature joined to the orbital motion of surface electrons around nanometric to micrometric domains induces giant anisotropic orbital momenta that are ultimately responsible for the magnetic signal and magnetic behavior of the samples.[9,34] These arguments have also been used to explain the physical mechanisms related to the magnetism of the thiol-capped Au NPs.[35] In our case, the contribution of the orbital moment to the magnetism of these Au NPs can be estimated from the XMCD results. Using the sum rules,[36,37] the ratio of the orbital to the spin magnetic moment $<\mu_L/\mu_S>$ was calculated to be 0.10. This value is not surprisingly high and cannot be taken as representative of a magnetic system led by the orbital momenta.[1] It is larger than those observed in orbital-quenched 3d transition metals but lower than, for example, the $<\mu_L/\mu_S>$ ratio measured in spin polarized Au atoms at the interfaces of Au/Co multilayers.[38] More enlightening is the comparison with the polyallyl amine hydrochloride (PAACH)-capped Au particles of similar size synthesized by Yamamoto et al.[39] The authors calculated for these NPs a $<\mu_L/\mu_S>$ ratio of 0.145, significantly higher than the 0.10 value observed in Au NPs studied in this paper. As a higher contribution of orbital momentum is associated with higher magnetic anisotropy, a stronger magnetic behavior would be expected from the PAACH-capped Au NPs. However, these NPs are superparamagnetic even at temperatures down to 2.6 K.

The directional and localized metal−S bond at the surface of the NPs and the sphere-like shape of the latter ones lead to an arrangement where all the magnetic moments would be orientated perpendicularly to the surface reaching, as a whole, a random high anisotropy orientation. In a system characterized by a considerable orbital magnetic contribution, the rotation of the angular momenta with an applied external magnetic field would require the rotation of the electric charge distribution linked to the directional metal−S bond at the surface of the NPs and a hysteresis loop featured by an unsaturated magnetic signal and a defined remanence to magnetization ratio of 1/2 would be expected, as it has been observed in thiol-capped Au NPs.[19] In contrast with this assumption, the Au, Ag, and Cu dodecanothiol-capped NPs studied in this paper present a saturated magnetic signal even from moderate applied fields, clearly indicating collectivity among the magnetic moments of the surface metal atoms. The origin of this collective state must be due to the coupling exchange among the spins of the located d electrons responsible for the magnetism in the samples. It has recently been pointed out theoretically that in certain circumstances spin−spin exchange interactions can prevail over the high anisotropy associated with orbital magnetic moments even in two-dimensional magnetic systems and so induce the alignment of the orbital moments through the strong spin−orbit coupling.[35]

Very few papers have been published up to now dealing with the magnetism of organically capped Au or very recently Ag NPs.[11,18−20,22,23,39,40] None of them reports the same magnetic behavior, including this one. The calculated values for the magnetic moments for the magnetic Au spread from 0.002 to 0.036 μ_B, much lower than the value of ∼0.3 μ_B calculated for the NPs studied in this paper. These different data, however, must not be taken as contradictory but as complementary. All of them reflect the generation of holes in the 5d energy level as a consequence of different bonds among the surface Au atoms and the different organic groups. The efforts must be center on the understanding of the chemical and physical mechanisms hidden behind the different chemical bonds.

In the present case, Au, Ag, and Cu were selected for comparison because their similar electronic structures, $nd^{10}(n+1)s^1$, similar chemical affinities, and same diamagnetic behavior of the bare bulk state. The capped NPs were synthesized under the same chemical recipe and the same synthesis conditions. The three samples show permanent magnetism at room temperature with high magnetic moments and basically similar magnetic characteristics. The thermogravimetry and ICP−MS results fit approximately in the relative quantities of the S atoms on the surface of the NPs. As can be observed in Table 1, the S/metal ratio at the surface is in our case ∼0.3, which indicates that each S atom would be linked to three surface metal atoms. This bond has been observed to be formed by chemisorption of alkanethiolates on monolayers of Au and Ag. The S atoms would lean into the hollow formed by adjacent atoms at the surface inducing σ- and π-bonding orbitals with the thiol specie.[41] The bonds adapt to the local symmetry of the hollow, which could cause the partial quenching of the magnetic orbits of the metal atoms at the surface of the NPs.

Acknowledgment. Financial support from the Spanish CICYT under Grant No. MAT2006-12743, by University of the Basque Country UPV/EHU-GIU06/59 and by Australian Research Council. E.G. thanks the Basque Government for financial support and J.S.G. the Spanish Education and Science Ministry (MEC) for support under the program Movilidad de Profesores de Universidad. The XMCD experiments at SPring-8 were performed with the approval of the Japan Synchrotron Radiation Research Institute (JASRI) as a Nanotechnology Support project of the Japanese Ministry of Education, Culture, Sports, Science and Technology (Proposal No. 2006B1536). The authors also thank the Australian Institute of Nuclear Science and Engineering for the neutron facility. J.S.G. is indebted to Prof. A. Hernando for useful suggestions.

Supporting Information Available: Synthesis and experimental methods. This material is available free of charge via the Internet at http://pubs.acs.org.

References

(1) Gambardella, P. *Nature* **2002**, *416*, 301−304.
(2) Zeng, H.; Li, J.; Liu, J. P.; Wang, Z. L.; Sun, S. *Nature* **2002**, *420*, 395−398.
(3) Nobusada, K. *J. Phys. Chem. B* **2004**, *108*, 11904−11908.
(4) Liu, H.; Mun, B. S.; Thomton, G.; Isaacs, S. R.; Shon, Y. S.; Ogletree, D. F.; Salmeron, M. *Phys. Rev. B* **2005**, *72*, 155430−155434.
(5) Zhang, P.; Sham, T. K. *Phys. Rev. Lett.* **2003**, *90*, 245502−245505.
(6) López-Cartés, C.; Rojas, T. C.; Litrán, R.; Martínez-Martínez, D.; de la Fuente, J. M.; Penadés, S.; Fernández, A. *J. Phys. Chem. B* **2005**, *109*, 8761−8799.

(7) Leff, D. V., Brandt, L.; Heath, J. R. *Langmuir* **1996**, *12*, 4723−4730.
(8) Boyen, H.-G.; Kästle, G.; Weigl, F.; Koslowski, B.; Dietrich, C.; Ziemann, P.; Spatz, J. P.; Riethmüller, S.; Hartmann, C.; Möller, M.; Schmid, G.; Garnier, M. G.; Oelfhafen, P. *Science* **2002**, *297*, 1533−1536.
(9) Jiang, G.; Wang, L.; Chen, T.; Yu, H.; Chen, C. *Mater. Chem. Phys.* **2006**, *98*, 76−82.
(10) Brust, M.; Walker, M.; Bethell, D.; Schiffrin. D. J.; Whyman, R. *J. Chem. Soc., Chem. Commun.* **1994**, *1994*, 801−802.
(11) de la Presa, P.; Multigner, M.; de la Venta, J.; García, M. A. *J. Appl. Phys.* **2006**, *100*, 123915−123920.
(12) Schaaff, T. G.; Whetten, R. L. *J. Phys. Chem. B* **2000**, *104*, 2630−2641.
(13) García, M. A.; Merino, J. M.; Fernández Pinel, E.; Quesada, A.; de la Venta, J.; Ruíz González, M. L.; Castro, G. R.; Crespo, P.; Llopis, J.; González-Calbet, J. M.; Hernando, A. *Nano Lett.* **2007**, *7*, 1489−1494.
(14) Litrán, R.; Sampedro, B.; Rojas, T. C.; Multigner, M.; Sánchez-López,J. C.; Crespo, P.; López-Cartes, C.; García, M. A.; Hernando, A.; Fernández, A. *Phys. Rev. B* **2006**, *73*, 054404−054410.
(15) Xiao, Y.; Patolsky, F.; Katz, E.; Hainfeld, J. F.; Willner, I. *Science* **2003**, *299*, 1877−1881.
(16) Jadzinsky, P. D.; Calero, G.; Ackerson, C. J.; Bushnell, D. A.; Kornberg, R. D. *Science* **2007**, *318*, 430−433.
(17) Carmeli, I.; Leitus, G.; Naaman, R.; Reich, S.; Vager, Z. *J. Chem. Phys.* **2003**, *118*, 10372−10375.
(18) Dutta, P.; Pal, S.; Seehra, M. S.; Anand, A.; Roberts, C. B. *Appl. Phys. Lett.* **2007**, *90*, 213102.
(19) Crespo, P.; Litrán, R.; Rojas, T. C.; Multigner, M.; de la Fuente, J. M.; Sánchez-López, J. C.; García, M. A.; Hernando, A.; Penedés, S.; Fernández, A. *Phys. Rev. Lett.* **2004**, *93*, 087204−087207.
(20) de la Venta, J.; Pucci, A.; Fernández Pinel, E.; García, M. A.; de Julián Fernández, C.; Crespo, P.; Mazzoldi, P.; Ruggeri, G.; Hernando, A. *Adv. Mater.* **2007**, *19*, 875−877.
(21) Goikolea, E. Synthesis, characterization and study of the magnetic properties of dodecanothiol capped nanoparticles. Dissertation for Bachelor's Degree, University of the Basque Country, Bilbao, Spain, 2005.
(22) Suber, L.; Fiorani, D.; Scavia, G.; Imperatori, P. *Chem. Mater.* **2007**, *19*, 1509−1517.
(23) Crespo, P.; García, M. A.; Fernández Pinel, E.; Multigner, M.; Alcántara, D.; de la Fuente, J. M.; Penadés, S.; Hernando, A. *Phys. Rev. Lett.* **2006**, *97*, 177203−177206.
(24) García, M. A.; de la Venta, J.; Crespo, P.; Llopis, J.; Penadés, S.; Fernández, A.; Hernando, A. *Phys. Rev. B* **2005**, *72*, 241403(R)−241406(R).
(25) Mulder, F. M.; van der Zeeuw, E. A.; Thiel, R. C.; Schmid, G. *Solid State Commun.* **1993**, *85*, 93−97.
(26) Paulus, P. M.; Goossens, A.; Thiel, R. C.; van der Kraan, A. M.; Schmid, G.; de Jongh, L. J. *Phys. Rev. B* **2001**, *64*, 205418/1−205418/18.
(27) González, C.; Simón-Manso, Y.; Marquez, M.; Mujica, V. *J. Phys. Chem. B* **2006**, *110*, 687−691.
(28) van Leeuwen, D. A.; van Ruitenbeek, J. M.; de Jongh, L. J.; Ceriotti, A.; Pacchioni, G.; Häberlen, O. D.; Rösch, N. *Phys. Rev. B* **1994**, *73*, 1432−1435.
(29) Ikeda, K.; Kobayashi, Y.; Negishi, Y.; Seto, M.; Iwasa, T.; Nobusada, K.; Tsukuda, T.; Kojima, N. *J. Am. Chem. Soc.* **2007**, *129*, 7230−7231.
(30) Parish, R. V. *Mössbauer Spectroscopy Applied to Inorganic Chemistry*; Long, G. J., Ed.; Springer: New York, 1985; Vol. I, pp 527−617.
(31) Cohen, R. L.; Wernick, J. H.; West, K. W.; Sherwood, R. C.; Chin, G. Y. *Phys. Rev.* **1969**, *188*, 684−691.
(32) Smit, H. H. A.; Thiel, R. C.; de Jongh, L. J.; Schmid, G.; Klein, N. *Solid State Commun.* **1988**, *6*, 915−920.
(33) Punnoose, A.; Magnone, H.; Seehra, M. S.; Bonevich, J. *Phys. Rev. B* **2001**, *64*, 174420−174427.
(34) Hernando, A.; Crespo, P.; García, M. A.; Fernández Pinel, E.; de la Venta, J.; Fernández, A.; Penadés, S. *Phys. Rev. B* **2006**, *74*, 052403−052406.
(35) Hernando, A.; Crespo, P.; García, M. A. *Phys. Rev. Lett.* **2006**, *96*, 057206−057209.
(36) Thole, B. T.; Carra, P.; Sette, F.; van der Laan, G. *Phys. Rev. Lett.* **1992**, *68*, 1943−1946.
(37) Carra, P.; Thole, B. T.; Altarelli, M.; Wang, X. *Phys. Rev. Lett.* **1993**, *70*, 694−697.
(38) Wilhelm, F.; Angelakeris, M.; Jaouen, N.; Poulopoulos, P.; Papaioannou, E. T.; Mueller, C.; Fumagalli, P.; Rogalev, A.; Flevaris, N. K. *Phys. Rev. B* **2004**, *69*, 220404(R)−220407(R).
(39) Yamamoto, Y.; Miura, T.; Suzuki, M.; Kawamura, N.; Miyagawa, H.; Nakamura, T.; Kobayashi, K.; Teranishi, T.; Hori, H. *Phys. Rev. Lett.* **2004**, *93*, 116801−116804.
(40) Hori, H.; Yamamoto, Y.; Iwamoto, T.; Miura, T.; Teranishi, T.; Miyake, M. *Phys. Rev. B* **2004**, *69*, 174411−174415.
(41) Sellers, H.; Ulman, A.; Shnidman, Y.; Eilers, J. E. *J. Am. Chem. Soc.* **1993**, *115*, 9389−9401.

NL073129G